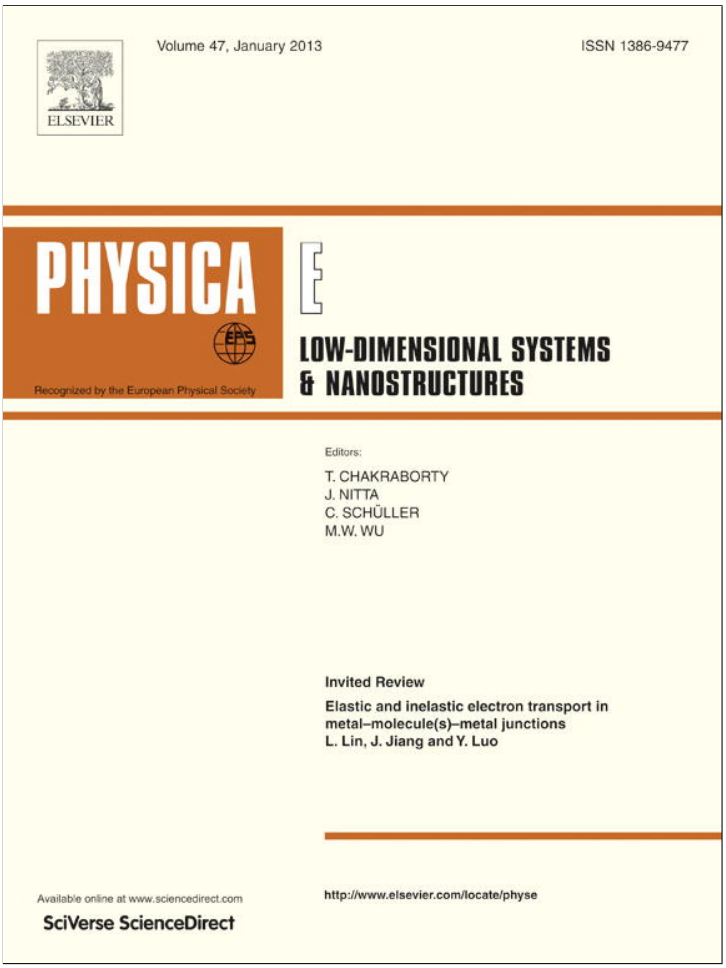

Physica E 47 (2013) 51–58

Contents lists available at SciVerse ScienceDirect

Physica E

journal homepage: www.elsevier.com/locate/physe

Efficiency improvement of light-emitting diodes with a developed electron blocking layer structure and its optimization

Tian-Hu Wang [a,b], Jin-Liang Xu [a,b,*], Xiao-Dong Wang [a,c,**]

[a] State Key Laboratory of Alternate Electrical Power System with Renewable Energy Sources, North China Electric Power University, Beijing 102206, China
[b] Beijing Key Laboratory of New and Renewable energy, North China Electric Power University, Beijing 102206, China
[c] Beijing Key Laboratory of Multiphase Flow and Heat Transfer for Low Grade Energy, North China Electric Power University, Beijing 102206, China

HIGHLIGHTS

- The internal quantum efficiency (IQE) of light-emitting diodes (LEDs) was studied.
- An $Al_xGa_{1-x}N$/GaN multi-quantum-barrier was added as the electron blocking layer.
- The structure parameter was optimized.
- The IQE is increased to 63.7% after optimization.

GRAPHICAL ABSTRACT

A developed electron blocking layer was studied and its structure parameters were optimized. The IQE is significantly increased for the optimized structure parameters. Effect of the Al compositions on IQEs for SB-EBL and MQB-EBL.

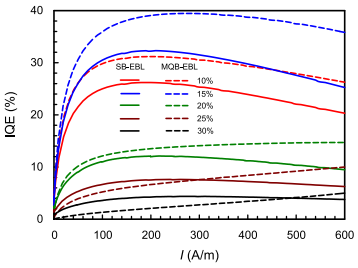

ARTICLE INFO

Article history:
Received 23 December 2011
Received in revised form
12 September 2012
Accepted 26 September 2012
Available online 12 October 2012

ABSTRACT

We study the internal quantum efficiency (IQE) of light-emitting diodes (LEDs) with an added $Al_xGa_{1-x}N$/GaN multi-quantum-barrier as the electron blocking layer (EBL) and optimize the structure parameter. Comparison was performed under same running conditions for LEDs with a single-barrier EBL (conventional design) and multi-quantum-barrier EBL. The numerical simulation shows that the IQE is significantly increased to 63.7% for the optimized structure parameters due to the modified energy band diagrams which are responsible for the enhanced carrier concentration in the active region.

1. Introduction

Recently, the III-nitride-based LEDs are widely used due to the low energy consumption, long lifetime and compact size [1–4]. Applications include full-color displays, automotive headlights, general lighting to replace cold cathode fluorescent lump, etc. For high power applications, LEDs operate at high current densities, yielding remarkable efficiency droops. The reduced electron injection efficiency into quantum wells by electron leakage due to the low hole mobility in p-type AlGaN layers accounts for the reduction of the LED efficiency.

For the purpose of electron injection efficiency improvement, an EBL inserted between the multi-quantum wells and the p-type layer, is attractive to suppress the overflow of electrons from quantum wells into the p-type layer [5–8]. At this stage, the AlGaN EBL has been widely applied in III-nitride-based LEDs. However, it is known that the large polarization field in the AlGaN

* Corresponding author at: North China Electric Power University, State Key Laboratory of Alternate Electrical Power System with Renewable Energy Sources, Beinong Road, Beijing 102206, China. Tel./fax: +86 10 61772268.
** Corresponding author at: North China Electric Power University, State Key Laboratory of Alternate Electrical Power System with Renewable Energy Sources, Beinong Road, Beijing 102206, China. Tel./fax: +86 10 62321277.
E-mail addresses: xjl@ncepu.edu.cn (J.-L. Xu), wangxd99@gmail.com (X.-D. Wang).

1386-9477/$ - see front matter © 2012 Elsevier B.V. All rights reserved.
http://dx.doi.org/10.1016/j.physe.2012.09.024

EBL decreases the effective barrier height for electrons, and the hole injection is degraded by the barrier height between the last barrier and the EBL [9]. Thus new designs are reported to overcome such shortcomings. Recently, the polarization-matched InAlN or AlInGaN EBLs were proposed to replace the AlGaN EBL and they are proved to be more effective for electron confinement. However, it is difficult to fulfill the epitaxy and the crystal quality of the subsequent p-type GaN layer is degraded. Alternatively, a multi-quantum-barrier EBL (MQB-EBL) can also be used to replace the AlGaN EBL to suppress the electron overflow. Iga et al. [10] theoretically predicted that the multi-quantum-barrier can raise the "effective" barrier height in 1986 firstly. Such effect was experimentally verified for the red laser diodes with a new GaInP/AlInP MQB by Kishino et al. [11] in 1991. Since then, the new Mg-doped AlGaN/GaN MQB structure have showed a significant improvement for doping efficiency which is ten times higher than that of the p-type GaN [12–14]. However, Refs. [12–14] only studied the material characteristics, which had not been used for the LEDs. Following then, various MQB-EBLs have been proposed and applied in LED chips. Hirayama et al. [15] reported significantly increased external quantum efficiency with an AlGaN/AlGaN MQB-EBL. Kim et al. [16] introduced an AlGaN/GaN/InGaN superlattice to suppress the electron overflow and enhance the hole transport to InGaN quantum wells. Wang et al. [17] explore the effect of $Al_{0.3}GaN_{0.7}$/GaN short-period superlattice-inserted structures in the GaN under-layer on the performance of multi-quantum well LEDs, in their work the superlattice structure was not used as EBL. Though these investigations have confirmed that the MQB structures is effective to improve the LED efficiency at high current densities, these designs only focus on one degree of freedom such as the energy gap, equivalently, the Al molar fraction. The MQB structures reported in the literature are listed in Table 1, which help readers to understand the differences between the past study and the present study.

To the authors' knowledge, fewer studies have been performed on the structure optimization. We note that there are many parameters of MQB structure influencing the LED performance. These parameters are coupled with each other. The structure optimization is quite necessary for LED practical applications. Besides, the concentration of each species is important to affect the LED performance. For instance, Hirayama et al. [15] recommended the $Al_{0.95}Ga_{0.05}N/Al_{0.77}Ga_{0.23}N$ MQB structure. It is not known that the 95% aluminum concentration is the optimized one. Thus the species concentration should be further optimized.

The objective of this paper is to identify the effect of various parameters of the $Al_xGa_{1-x}N$/GaN MQB-EBL on the IQE for LEDs using a non-isothermal multi-physics coupling model, based on which an optimal $Al_xGa_{1-x}N$/GaN MQB-EBL structure is presented. Comparison was performed under same running conditions for LEDs with a single-barrier EBL (conventional design) and multi-quantum-barrier EBL. The mechanisms that new MQB-EBL structure improves the LED performance are also discussed.

2. Device structure and simulation parameters

The LED is grown on a *c*-plane 100 μm thick sapphire substrate, followed by a 50 nm thick un-doped GaN buffer layer. Next, a n-type GaN layer (3 μm thick, doping concentration of 5×10^{18} cm^{-3}) is deposited on the buffer layer. The active region consists of five 4 nm thick un-doped $In_{0.08}Ga_{0.92}N$ quantum wells sandwiched by six 10 nm thick $In_{0.02}Ga_{0.98}N$ barriers. On the top of the active region, an EBL is deposited. Finally, the chip is completed with a 250 nm thick p-type GaN cap layer with a doping concentration of 1.2×10^{18} cm^{-3}. The substrate and active region have widths of 300 μm and 200 μm, respectively. The widths are 50 μm and 70 μm for the n-contact and p-contact respectively. Fig. 1 shows the schematic diagram of the studied LED chip.

To investigate the effect of MQB-EBL on the electron overflow from active region to p-type layer, two different EBLs were used deliberately after the growth of the $In_{0.02}Ga_{0.98}N/In_{0.08}Ga_{0.92}N$ quantum wells. The first is an $Al_xGa_{1-x}N$ single-barrier EBL (SB-EBL) with Mg doped. The second is the MQB-EBL with Mg doped. $Al_xGa_{1-x}N$ and GaN are called quantum barrier and quantum well, respectively. Because the Al composition, p-doping level, barrier-to-well thickness ratio, thickness of barrier–well-pair and number of $Al_xGa_{1-x}N$/GaN pairs influence the MQB-EBL performance, a comprehensive parametric study shown in Table 2 is performed to obtain optimal IQE for LEDs.

Initially the Al composition over a range of 10–30% was optimized with a Mg-doped concentration of 3×10^{17} cm^{-3}, thickness ratio of barrier-to-well of 2.40, barrier-well-pair thickness of 20 nm, and pair number of 4. Then the Mg-doped concentration over a range of 1×10^{17}–1×10^{18} cm^{-3} was optimized with the constant values of the rest three parameters using the above optimized Al composition. The thickness ratio of barrier-to-well (0.13–7.5), barrier-well-pair thickness (4.25–25.50 nm) and pair

Table 1
MQB structures used in Refs. [10–17] and the present study.

References	Structure details	Comments
Iga et al. [10]	MQB theoretical model	No applications in LED.
Kishino et al. [11]	GaInP/AlInP MQB	The enhanced carrier confinement effect of MQB in lasers is demonstrated.
Kozodoy et al. [12]	$Al_{0.2}Ga_{0.8}N$/GaN supperlattice	High-p-type conductivity of Mg-doped $Al_{0.2}Ga_{0.8}N$/GaN superlattices is demonstrated.
Kim et al. [13]	$Al_{0.17}Ga_{0.83}N/Al_{0.36}Ga_{0.64}N$ supperlattice	The structure exhibits strong p-type conductivity.
Wang et al. [14]	$Al_{0.14}GaN_{0.86}$/GaN superlattices with AlN interlayer	The structure markedly decreases the effective acceptor activation energy which is beneficial for high p-type conductivity.
Hirayama et al. [15]	$Al_{0.95}Ga_{0.05}N/Al_{0.77}Ga_{0.23}N$ MQB	Significant increase in the external quantum efficiency was observed.
Kim et al. [16]	AlGaN/GaN/InGaN supperlattice	Optical output power with stable temperature characteristic can be achieved in InGaN based LED by introducing AlGaN/GaN/InGaN supperlattice in EBL.
Wang et al. [17]	$Al_{0.3}Ga_{0.7}N$/GaN short-period-superlattice-inserted structures	The structure enables the improved LED performance (not used as EBL).
Present study	$Al_xGa_{1-x}N$/GaN MQB-EBL	The general idea of the proposed MQB structure is similar to the above studies, but we focus on the concentration effect of each species and all the related parameters on the LED performance. The optimization of these parameters is performed.

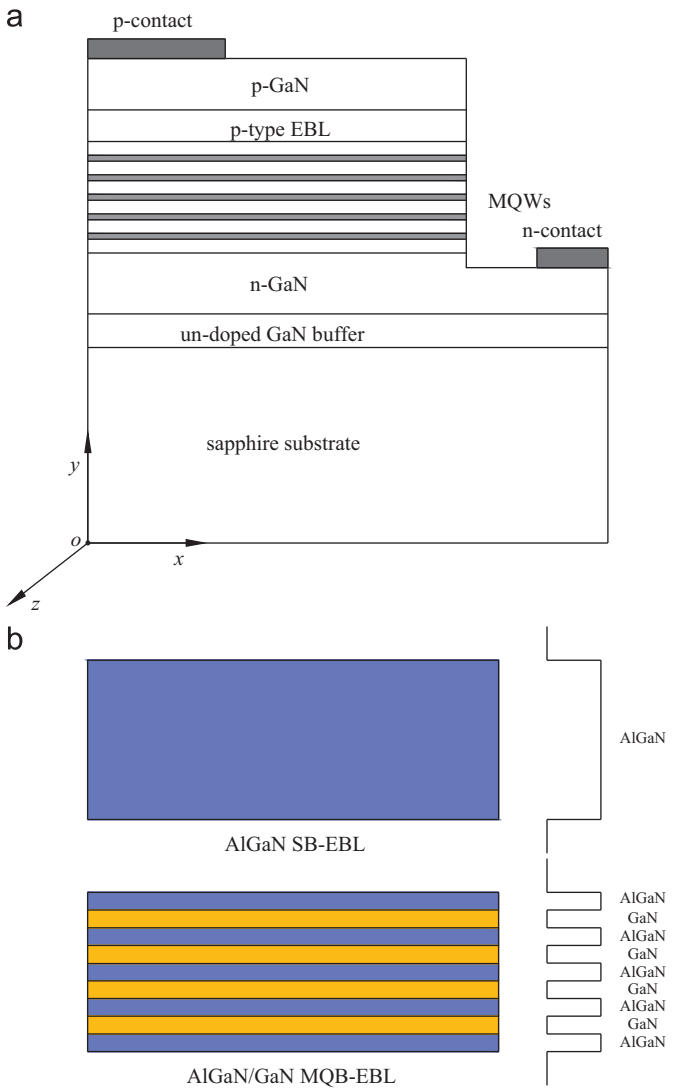

Fig. 1. Schematic diagram of the LED. (a) The entire LED chip; (b) two different EBL structures.

Table2
Parameters for MQB-EBL for the optimization computations.

Al composition (%)	p-doping level (m^{-3})	Barrier-to-well thickness ratio	Barrier–well-pair thickness (nm)	Barrier–well-pair number
10	1×10^{17}	0.13	4.25	4
15	3×10^{17}	0.42	8.50	8
20	5×10^{17}	1.00	12.75	12
25	8×10^{17}	2.40	17.00	16
30	1×10^{18}	7.50	21.25	20
–	–	–	25.50	24

number (4–24) of MQB-EBL are optimized in a similar way. Thus a set of optimal parameters are obtained.

3. Numerical model

A complete multi-physics-field-simulation model is used here, incorporating the thermal generation and dissipation effect considered by energy equation over an entire LED. The model assumes that: (1) the LED chip operates in a steady state, (2) there is no thermal contact resistance at the hetero-interface between two adjacent layers and temperature and heat flux are continuous across such internal interfaces, and (3) the isothermal boundary condition is used on the bottom substrate surface with a temperature of $T=313$ K. Other surfaces enclosing the LED chip are adiabatic. The model includes the Poisson's equation for potential distribution, current continuity equations for transport and distribution of electrons and holes in LED structure, energy equation for temperature distribution. We solve the Poisson and Schrödinger equations for the carrier discrete energy levels and wave functions in quantum wells self-consistently. Besides, the energy band structures are calculated based on a self-consistent 6-band $\boldsymbol{k\cdot p}$ method for wurtzite semiconductor [18]. Most of parameters for material properties such as GaN, AlGaN and InGaN are cited from Ref. [19]. The governing equations and other relevant physicochemical parameters in governing equations can be found in Ref. [20].

4. Results and discussion

4.1. Alloy composition

Fig. 2 shows the effect of Al composition on the IQE for SB-EBL and MQB-EBL. The Mg-doped level and EBL thickness are 3×10^{17} cm^{-3} and 20 nm respectively for both structures. The barrier-to-well thickness ratio is 2.4 with the barrier-well-pair number of 4 for the MQB-BEL. It is found that the IQE of MQB-EBL is higher than that of SB-EBL if the Al composition is less than 20%. The better performance of MQB-EBL exists only at high injection current if the Al composition is larger than 20%. In the latter case the IQE of MQB-EBL is increased slightly with increases in injection currents, indicating that the efficiency droop does not occur.

The higher IQE of MQB-EBL than that of SB-EBL at Al compositions less than 20% is explained as follows. On the one hand, the AlGaN film generally suffers from lower hole concentration caused by the higher Mg acceptor activation energy, yielding the lower p-type conductivity. Because the MQB-EBL structure includes p-GaN layers, the activation energy is lower for Mg dopant in the GaN than that in the AlGaN. The Mg dopant is more easily activated in the p-type AlGaN/GaN MQB-EBL than that in the single-barrier AlGaN EBL. Thus the effective barrier height of AlGaN/GaN MQB-EBL is higher than that of the AlGaN SB-EBL (Fig. 3). On the other hand, based on the reflectivity ratio and transition ratio of electrons in multi-quantum-barrier computed by the one-dimensional Schrödinger equation (Iga [10]), the

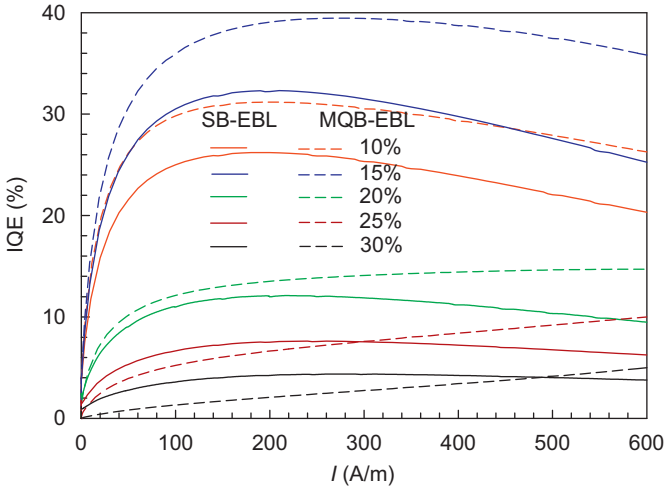

Fig. 2. Effect of the Al compositions on IQEs for SB-EBL and MQB- EBL.

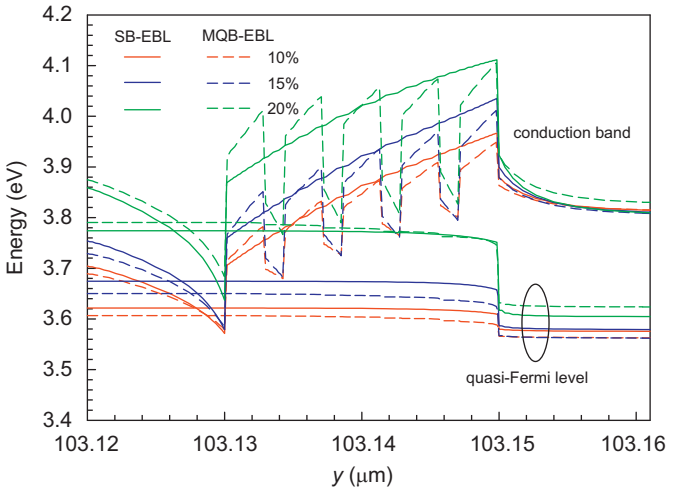

Fig. 3. Conduction band for SB-EBL and MQB-EBL at various Al compositions at the current of 400 A/m.

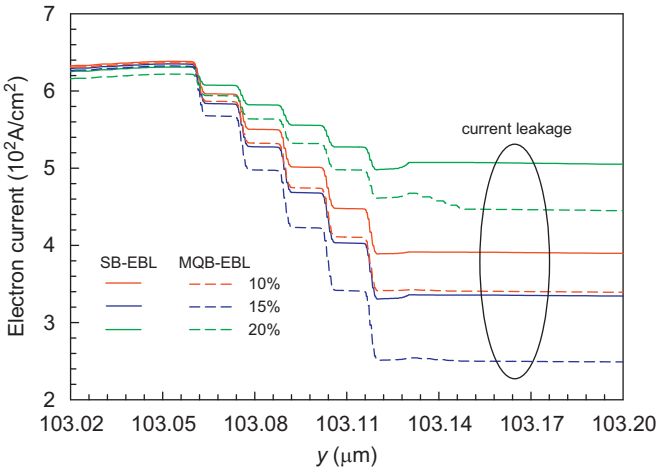

Fig. 4. Current leakage for SB-EBL and MQB-EBL at various Al compositions for the current of 400 A/m.

electron reflectivity is significantly increased in MQB-EBL than that in SB-EBL. Correspondingly, the effective barrier height is increased in MQB-EBL. Thus the MQB-EBL structure enhances the confinement of electrons. Due to the increased barrier height and reflectivity ratio of electrons, the current leakage in MQB-EBL is significantly smaller than that in the SB-EBL (Fig. 4). It is also noted that an important reason for the reduced recombination rates of electrons and holes in quantum wells is the great strain in SB-EBL structures. But the AlGaN/GaN MQB-EBL has smaller strain than the SB-EBL structure [21], improving the recombination rates in quantum wells.

The barrier heights of conduction band and valence band are further increased with increases in the Al compositions beyond the value of 20%. It is difficult for electrons to overflow from quantum well to p-type layer due to the low electron concentration and energy level at low current densities. Under such circumstance the injection efficiency of holes is more important than the overflow of electrons to influence the IQE. The higher barrier height in the valence band in MQB-EBL prevents the holes from injecting into quantum wells, causing lower IQE for MQB-EBL than that for SB-EBL. At high current densities, more electrons hold high energy levels due to the energy band filling effect. The overflow of electrons from quantum wells to p-type layer becomes the dominant mechanism to affect the IQE. Thus the MQB-EBL has better performance than the SB-EBL.

Seeing from Fig. 2, the Al compositions have similar influences on IQEs for both SB-EBL and MQB-EBL, i.e., the IQEs are increased and then decreased with continuous increases in the Al compositions. The optimal Al composition is 15%. The existence of an optimal Al composition is attributed to that the electron overflow is determined by two competitive mechanisms: one is the barrier height of conduction band and the other is the hole concentration in the p-type layer. With increases in the Al composition, the increased barrier height of conduction band is helpful to prevent electrons from escaping from quantum wells to p-type layer. On the other hand, the higher Al composition induces higher activation energy and lower activation ratio for Mg in EBL. Meanwhile, the higher Al composition also raises the barrier height of valance band. Both the above two factors prevent holes injecting from p-type layer into quantum wells, resulting in the higher hole concentration in p-type layer. Han et al. [22] noted that the higher hole concentration in p-type layer accelerates the escaping of electrons from quantum wells to p-type layer. Therefore the current leakage is controlled by the above two competitive factors. Fig. 4 gave the strong evidence for the above analysis. In summary, the effect of the increased barrier height of conduction band on the escaping of electrons is important to influence the IQE at low Al compositions over the range of 10–15%. But the effect of hole concentration in p-type layer on the escaping of electrons becomes important at higher Al composition such as in the range of 15–30%. Fig. 5 further verifies the above analysis. At the current of 400 A/m, both the concentrations of electrons and holes attain maximum values at the Al composition of 15%. For the quantum well close to the EBL, the concentrations of electrons are increased by 15.97% and 37.58% at the Al composition of 15% than those at the Al composition of 10% and 20% respectively for MQB-EBL structure. Meanwhile, the concentrations of holes are increased by 21.20% and 70.48% at the Al composition of 15% than those at the Al composition of 10% and 20% respectively.

4.2. p-doping level

The doping level is another important parameter to affect the EBL performance. Fig. 6 shows the effect of Mg-doped level on IQEs for both SB-EBL and MQB-EBL at the same Al composition of 15%, coming from the optimized value in Section 4.1. The EBL thickness is 20 nm, and the barrier-to-well thickness ratio is 2.40 with the pair number of 4 for MQB-BEL. As shown in Fig. 6, the IQEs are increased with increases in the doping levels for both SB-EBL and MQB-EBL, and the MQB-EBL performance is better than the SB-EBL. As reported by Chiaria et al. [23], there are two reasons for the improved IQE by increasing the doping levels: (1) the higher doping level makes more holes available for recombining with electrons in the quantum wells (Fig. 7) and (2) the highly doped EBL causes the quasi-Fermi energy level of holes to approach the valance band edge, mitigating the valence band offset (Fig. 8a). Fig. 8 shows the energy band diagram at the p-doping levels of 1×10^{17}, 5×10^{17} and 1×10^{18} cm^{-3}, respectively. Because it is much easier for the Mg-acceptor to be activated in MQB-EBL than that in SB-EBL, the barrier height of conduction band is increased faster in MQB-EBL than that in SB-EBL with increases in the doping levels (Fig. 8b). Thus it is more effective for the MQB-EBL to inhibit the escaping of electrons and reduce the current leakage than that for SB-EBL when the doping levels are the same for both structures. Besides, the higher doping levels weaken the efficiency droop for both MQB-EBL and SB-EBL. Here the degree of efficiency droop is defined as $(IQE_{max}-IQE_{I=600\ A/m})/IQE_{max}$. At the doping level of 5×10^{17} cm^{-3}, the degree of efficiency droop is 9.37% for MQB-EBL, which is lower than the value of 22.22% for SB-EBL. Because the doping level approaches the maximum limit of 10^{18} cm^{-3} for the EBL

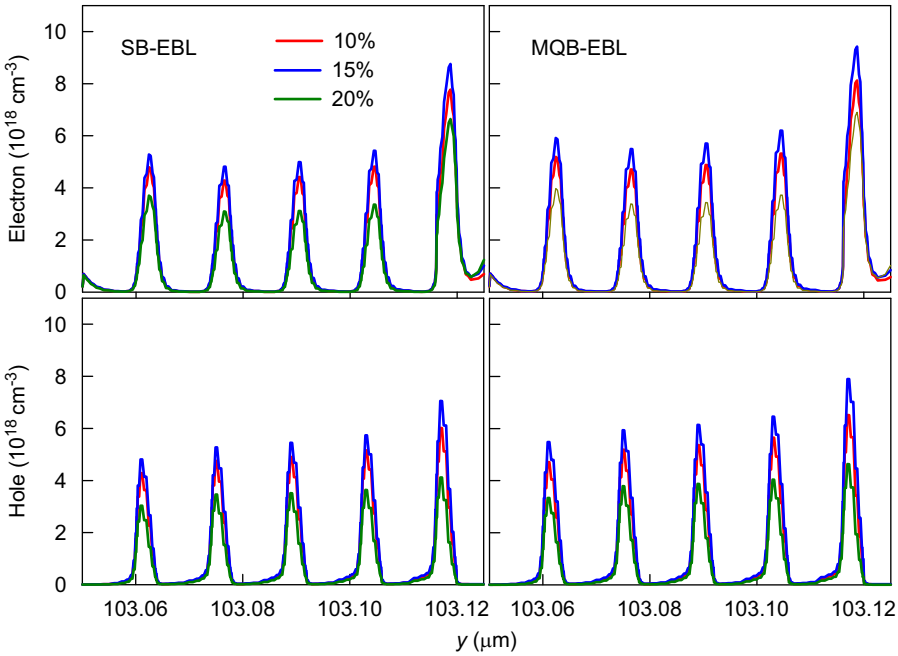

Fig. 5. Carrier concentrations for SB-EBL and MQB-EBL at various Al compositions for the injection current of 400 A/m.

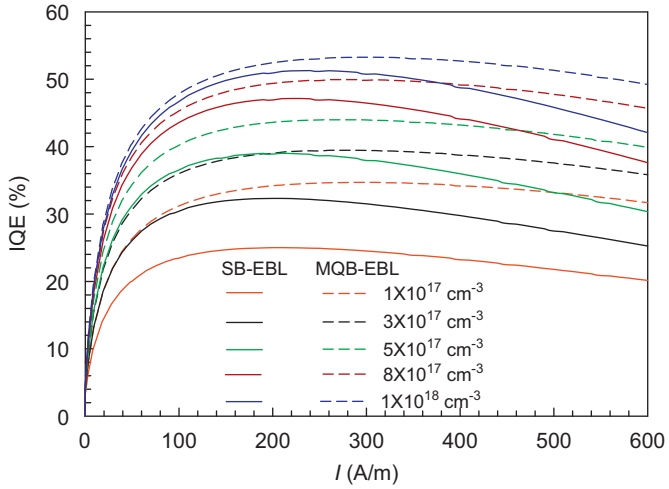

Fig. 6. Effect of p-doping levels on IQEs for SB-EBL and MQB-EBL.

[23], the IQE cannot be further improved for SB-EBL at this stage. But the IQE can be further increased for MQB-EBL under the doping level limit.

4.3. Barrier-to-well thickness ratio of MQB-EBL

In addition to the effect of the Al composition and doping level, the MQB-EBL performance is also strongly dependent on the structure parameters including the barrier-to-well thickness ratio, barrier–well-pair thickness and barrier–well-pair number. The available studies reported a scattered distribution of the barrier-to-well thickness ratios. Hirayama et al. [15] introduced an $Al_{0.95}Ga_{0.05}N/Al_{0.77}Ga_{0.23}N$ MQB-EBL with the barrier-to-well thickness ratio of 2:1. Lee et al. [21] studied a four pairs $Al_{0.2}Ga_{0.8}N/GaN$ MQB-EBL with a constant barrier thickness of 3 nm. The thickness of the four wells was set as 0.5, 1.0, 1.5 and 2.0 nm, respectively. Lai et al. [24] studied an $Al_{0.2}Ga_{0.8}N/GaN$ MQB-EBL with the barrier-to-well thickness ratio of 0.86. Here we identify the effect of the barrier-to-well thickness ratios covering a wide range of 0.13–7.5 on the MQB-EBL performance to obtain the optimal value. For such computations, the barrier-well-pair thickness was 4.25 nm and the pair number was 4. Other parameters such as the Al composition and p-doping level are specified as 15% and 1×10^{18} cm^{-3} respectively, optimized from Sections 4.1 and 4.2.

Fig. 9 shows that the IQE is increased with decreases in the barrier-to-well thickness ratio, with the optimal ratio of 0.13. We explain the reason here. Fig. 10 identifies that the smaller barrier-to-well thickness ratio causes larger barrier height of the conduction band. For instance, the barrier height of the conduction band is 496.41 meV at the barrier-to-well thickness ratio of 0.13, which is larger than the value of 412.39 meV at the barrier-to-well thickness ratio of 7.5. Thus smaller barrier-to-well thickness ratio is helpful to inhibit the escaping of electrons more effectively. On the other hand, the barrier energy band is strongly bending at larger barrier-to-well thickness ratio. But the bending phenomenon is weakened at smaller barrier-to-well thickness ratio. The bending of the energy band, caused by the polarization at the interface between the quantum well and EBL, increases the quasi-Fermi energy level of electrons. Thus there are more electrons with high energy, enhancing the escaping of electrons.

4.4. Barrier–well-pair thickness of MQB-EBL

Fig. 11a shows the IQE versus the barrier–well-pair thicknesses of MQB-EBL. The computations were performed with the following optimized parameters: the Al composition of 15%, Mg doping level of 1×10^{18} cm^{-3}, barrier-to-well thickness ratio of 0.13. The pair number is assumed be to 4. Fig. 11b shows the IQE versus thickness of SB-EBL. For fair comparison, the Al composition, Mg doping level and total thickness in the SB-EBL are the same as that in the MQB-EBL. It can be seen that the IQE is increased monotonically with increases in the total EBL thickness for SB-EBL; however, there is only a marginal improvement with the total thickness larger than 88 nm. This finding is consistent with that reported by Ref. [23]. But for MQB-EBL, IQEs are increased to a maximum value and then are decreased with

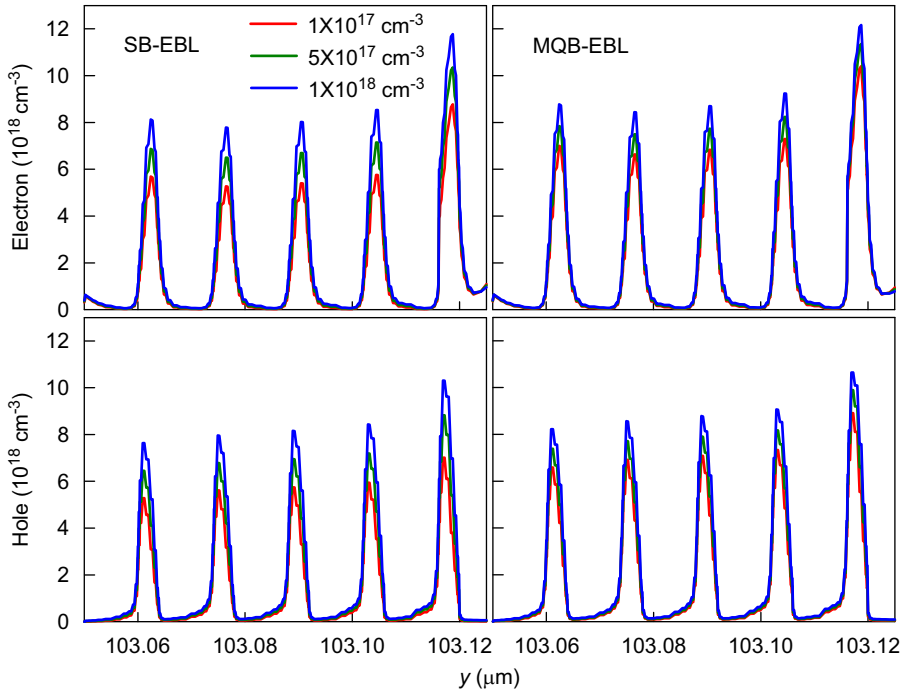

Fig. 7. Carrier concentrations for SB-EBL and MQB-EBL at various p-doping levels for the current of 600 A/m.

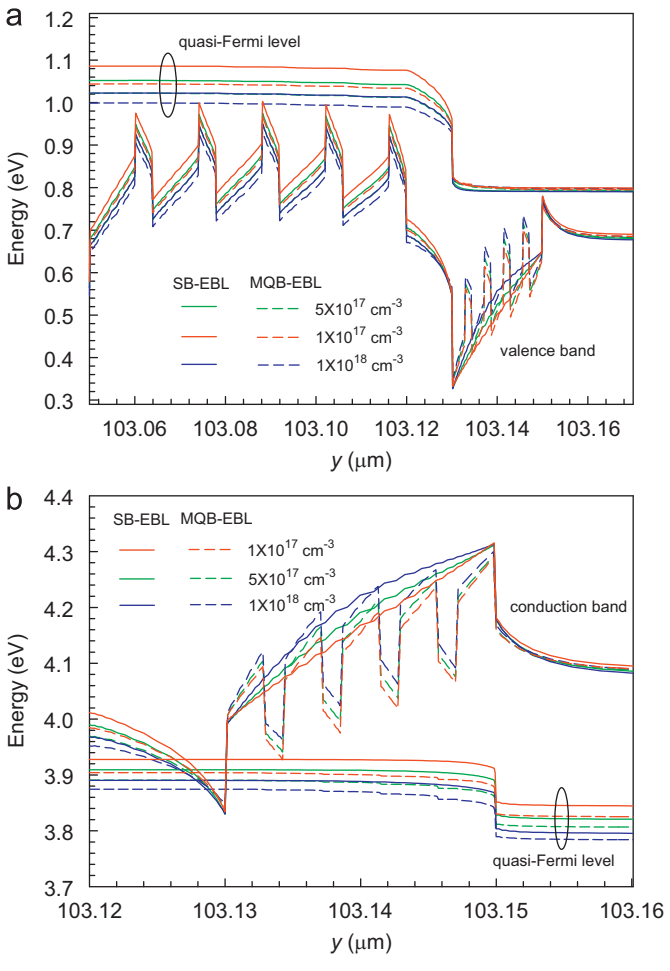

Fig. 8. Energy band diagrams for SB-EBL and MQB-EBL at various p-doping levels for current of 600 A/m. (a) Valence band; (b) conduction band.

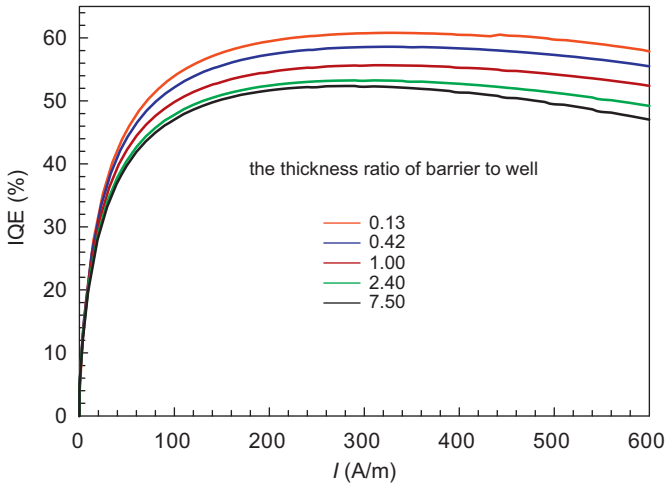

Fig. 9. Effect of the barrier-to-well thickness ratio on IQEs for SB-EBL and MQB-EBL.

continuous increases in the barrier–well-pair thicknesses. The optimal barrier–well-pair thickness is 8.5 nm with the maximum IQE of 61.63%, which is significantly larger than the maximum IQE value of 56.26% at the optimal thickness of 105 nm for SB-EBL. Besides, introducing the MQB-EBL structure weakens the efficiency droop phenomenon at high injection currents, which is benefit for the LED operation at high injection currents. Seeing from Fig. 12, the barrier height of conduction band are 489.52 meV, 504.09 meV and 443.43 meV at the barrier–well-pair thicknesses of 4.25 nm, 8.5 nm and 25.5 nm, respectively. Thus the maximum barrier height of conduction band takes place at the barrier–well-pair thickness of 8.5 nm, providing the maximum capability to inhibit the escaping of electrons. Besides, there is a strong band bending at the interface between the last barrier and EBL at the barrier–well-pair thickness of 25.5 nm,

which enhances the overflow of electrons and reduces the IQE, hence the IQE is obviously less than that of thickness 4.25 nm and 8.5 nm.

4.5. Barrier–well-pair number of MQB-EBL

Fig. 13 shows the effect of barrier–well-pair numbers on the IQEs. The computations were performed under the following optimized parameters: the Al composition of 15%, Mg doping level of $1\times10^{18}\,cm^{-3}$, barrier-to-well thickness ratio of 0.13 and barrier–well-pair thickness of 8.5 nm. The pair numbers are changed in the range of 4–24. There is a weak influence of the pair numbers on IQEs at the injection current smaller than 250 A/m, beyond which the effect of pair numbers becomes obvious. The IQEs for MQB-EBL are 61.63%, 63.15%, 63.61%, 63.74%, 63.76% and 63.73% at the pair numbers of 4, 8, 12, 16, 20 and 24, respectively if the injection current is 600 A/m. Thus it is concluded that further increases of the pair numbers beyond 12 has weak improvement on the IQEs. Fig. 14 demonstrates the band diagrams with the

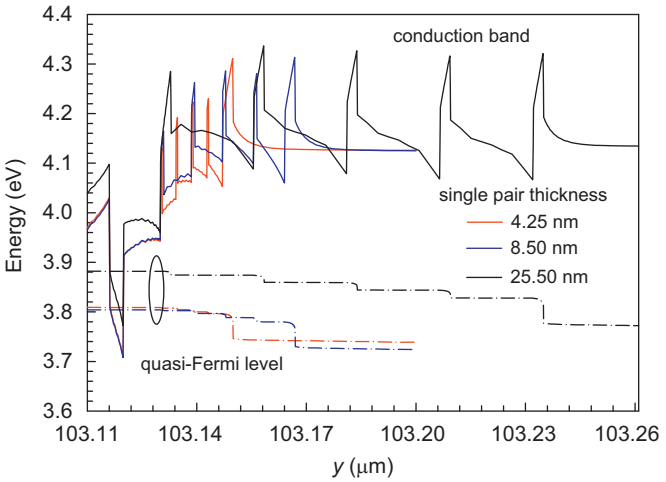

Fig. 12. Energy band diagrams for SB-EBL and MQB-EBL at various barrier–well-pair thicknesses for the current of 600 A/m.

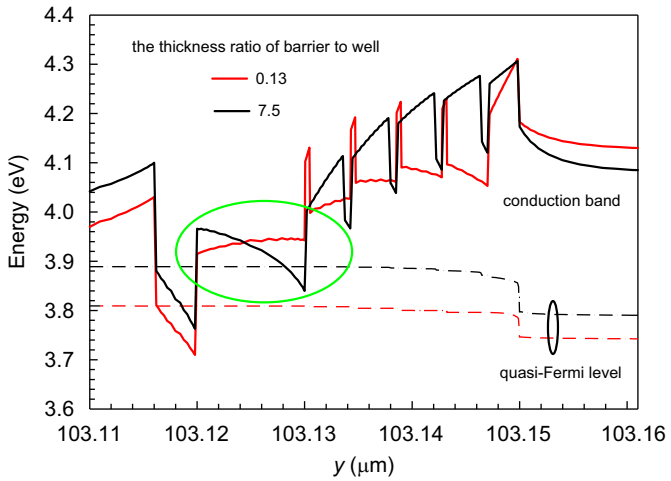

Fig. 10. Energy band diagrams for SB-EBL and MQB-EBL at various thickness ratio for the current of 600 A/m.

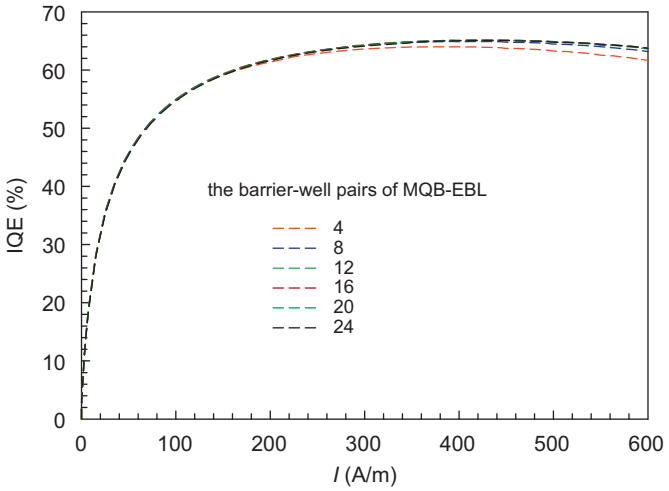

Fig. 13. IQEs versus the barrier–well-pair numbers for MQB-EBL.

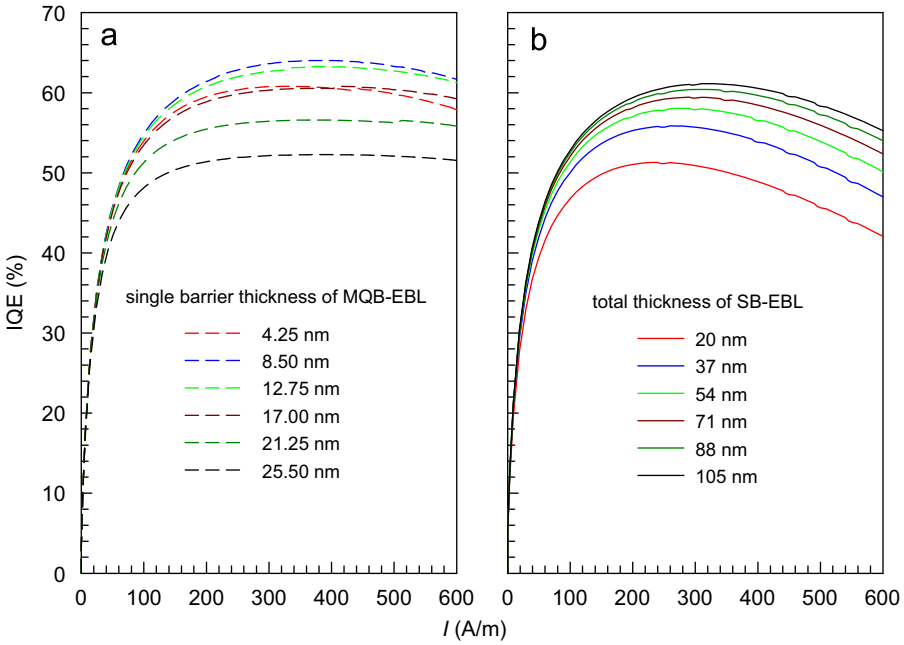

Fig. 11. Effect of barrier–well-pair thickness on IQEs. (a) Barrier–well-pair thickness on IQEs for MQB-EBL; (b) total thickness of SB-EBL on IQEs for SB-EBL.

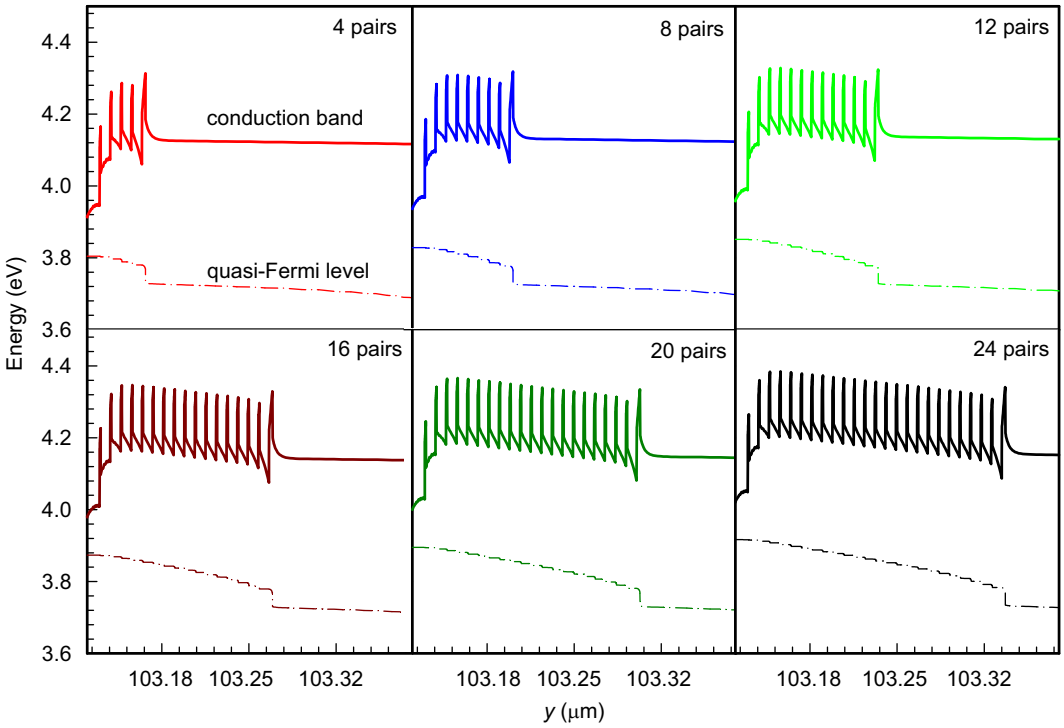

Fig. 14. Conduction band diagrams at various barrier–well-pair numbers for the current of 600 A/m.

barrier–well-pair number varied from 4 to 24. It can be seen that the barrier height is increased significantly for MQB-EBLs with various pair numbers which suppresses the electron overflow. The electron overflow is strong due to the tunneling effect for the pair number less than 12. The barrier is thick enough to impede tunneling current effectively for the pair number larger than 12. Under such circumstance the effect of pair number on the IQE is small.

5. Conclusions

A LED with added $Al_{1-x}Ga_xN$/GaN MQB-BEL was numerically studied. The structure parameters were optimized. The following conclusions can be drawn.

1. Because MQB-EBL has high electron reflection ratio, high effective barrier height and improved strain between quantum wells and EBL, concentrations of electrons and holes in the active region for MQB-EBL are significantly higher than those for SB-EBL, and the current leakage is greatly suppressed for MQB-EBL.
2. The internal quantum efficiency (IQE) for MQB-EBL can be reached as high as 63.76% at the optimal Al composition of 15% in $Al_{1-x}Ga_xN$ barrier layer, Mg-doped concentration of 1×10^{18} cm^{-3}, $Al_{1-x}Ga_xN$ barrier to GaN well thickness ratio of 0.13, barrier–well-pair thickness of 8.5 nm, and number of $Al_{1-x}Ga_xN$/GaN pairs of 12.
3. The significantly reduced overflow of electrons by the optimal band structure is responsible for the increased IQE for MQB-EBL.

Acknowledgment

This study was supported by the National Natural Science Foundation of China (Nos. U1034004 and 50825603) and by the Fundamental Research Funds for the Central Universities (Nos. 12QX14 and 11ZG01).

References

[1] M.R. Krames, O.B. Shchekin, R. Mueller-Mach, G.O. Mueller, L. Zhou, G. Harbers, M.G. Craford, IEEE Journal of Display Technology 3 (2007) 160.
[2] T. Fujii, Y. Gao, R. Sharma, E.L. Hu, S.P. DenBaars, S. Nakamura, Applied Physics Letters 84 (2004) 855.
[3] S. Nakamura, MRS Bulletin 34 (2009) 101.
[4] M.S. Shur, Proceedings of the IEEE 93 (2005) 1691.
[5] A. Chitnis, J.P. Zhang, V. Adivarahan, M. Shatalov, S. Wu, R. Pachipulusu, V. Mandavilli, M. Asif Khan, Applied Physics Letters 82 (2003) 2565.
[6] R.C. Tu, C.J. Tun, S.M. Pan, C.C. Chuo, J.K. Sheu, C.E. Tsai, G.C. Chi, IEEE Photonics Technology Letters 15 (2003) 1342.
[7] K.H. Kim, Z.Y. Fan, M. Khizar, M.L. Nakarmi, J.Y. Lin, H.X. Jiang, Applied Physics Letters 85 (2004) 4777.
[8] H. Hirayama, Journal of Applied Physics 97 (2005) 091101.
[9] C.H. Wang, C.C. Ke, C.Y. Lee, S.P. Chang, W.T. Chang, J.C. Li, Z.Y. Li, H.C. Yang, H.C. Kuo, T.C. Lu, S.C. Wang, Applied Physics Letters 97 (2010) 261103.
[10] K. Iga, H. Uenohara, F. Koyama, Electronics Letters 22 (1986) 1008.
[11] K. Kishino, A. Kikuchi, Y. Kaneko, I. Nomura, Applied Physics Letters 58 (1991) 1822.
[12] P. Kozodoy, M. Hansen, S.P. DenBaars, U.K. Mishra, Applied Physics Letters 74 (1999) 3681.
[13] J.K. Kim, E.L. Waldron, Y.L. Li, Th. Gessmann, E.F. Schubert, Applied Physics Letters 84 (2004) 3310.
[14] L. Wang, R. Li, D. Li, N. Liu, L. Liu, W. Chen, C. Wang, Z. Yang, X. Hu, Applied Physics Letters 96 (2010) 061110.
[15] H. Hirayama, Y. Tsukada, T. Maeda, N. Kamata, Applied Physics Express 3 (2010) 031002.
[16] K.S. Kim, J.H. Kim, S.J. Jung, Y.J. Park, S.N. Cho, Applied Physics Letters 96 (2010) 091104.
[17] C.L. Wang, M.C. Tsai, J.R. Gong, W.T. Liao, P.Y. Lin, K.Y. Yen, C.C. Chang, H.Y. Lin, S.K. Hwang, Materials Science and Engineering B 138 (2007) 180.
[18] S.L. Chuang, C.S. Chang, Physical Review B 54 (1996) 2491.
[19] I. Vurgaftman, J.R. Meyer, Journal of Applied Physics 94 (2003) 3675.
[20] T.H. Wang, X.D. Wang, J.L. Xu, Journal of Engineering Thermophysics 33 (2012) 647 (in Chinese).
[21] S.N. Lee, S.Y. Cho, H.Y. Ryu, J.K. Son, H.S. Peak, T. Sakong, T. Jang, K.K. Choi, K.H. Ha, M.H. Yang, O.H. Nam, Y. Park, Applied Physics Letters 88 (2006) 111101.
[22] S.H. Han, D.Y. Lee, S.J. Lee, C.Y. Cho, M.K. Kwon, S.P. Lee, D.Y. Noh, D.J. Kim, Y.C. Kim, S.J. Park, Applied Physics Letters 94 (2009) 231123.
[23] S. Chiaria, E. Furno, M. Goano, E. Bellotti, IEEE Transactions on Electron Devices 57 (2010) 60.
[24] M.J. Lai, L.B. Chang, R.M. Lin, C.S. Huang, Applied Physics Express 3 (2010) 072102.